AUCTORES
Globalize your Research

New Medical Innovations and Research

Sanmati Kumar Jain *

Open Access

Research Article

Bioisosteres of Pyridine Group: A Case Study with Rosiglitazone as PPAR-γ Activator in Diabetes Mellitus Treatment

Aashif Khan, Ajay Kumar Gupta, Sanmati Kumar Jain*

Educational Supervisor Certificate Rcp London and Accreditation Medical Examiner Member Rc Path London.

***Corresponding Author:** Sanmati Kumar Jain, Drug Discovery and Research Laboratory, Department of Pharmacy, Guru Ghasidas Vishwavidyalaya (A Central University), Bilaspur-495009, Chhattisgarh, India.

Received date: June 20, 2025; Accepted date: June 26, 2025; Published date: July 03, 2025

Citation: Aashif Khan, Ajay K. Gupta, Sanmati K. Jain, (2025), Bioisosteres of Pyridine Group: A Case Study with Rosiglitazone as PPAR-γ Activator in Diabetes Mellitus Treatment, *J New Medical Innovations and Research,* 6(7); **DOI:10.31579/2767-7370/150**

Abstract:

Diabetes is a significant global health challenge in the 21st century, impacting the health of individuals worldwide. Unhealthy lifestyle habits, influenced by genetic tendencies, are a significant contributor to the increasing prevalence of diabetes. Thiazolidinediones (TZDs) are type 2 diabetes medications that activate PPARs, promoting fatty acid storage in adipocytes, reducing fatty acid concentration in the bloodstream, and increasing glucose reliance. In this study, the authors implemented the bioisosterism approach to design novel analogues of Rosiglitazone (RGT), due to the presence of multiple toxicities associated with its treatment. A total of 191 pyridine bioisosteres, such as thiazolidine, phenoxy, and methoxyphenyl, were generated using the MolOpt tool. The newly designed compounds were assessed for their medicinal properties, pharmacokinetic (ADME) parameters, and toxicity profile through the ADMETLab 3.0 online tool. After screening, a total of 46 analogues found favorable drug-likeness, QED score, and Lipinski's rule. Notably, compounds RGT008, RGT029, RGT04, RGT05, RGT010, and RGT011 were identified as promising candidates based on their QED and MCE-18 scores. Additionally, compounds RGT011 and RGT021 exhibited reduced hepatotoxicity and cardiac toxicity compared to standard (RGT). The comprehensive analysis indicates that the compounds, specifically RGT05, RGT04, and RGT021, may be considered for additional assessment of the hypothesis as promising activators of PPAR-γ, serving as potential anti-diabetic agents.

Keywords: bioisosterism; pyridine bioisosteres; rosiglitazone; admet; diabetes mellitus

1.Introduction

Diabetes is recognized as one of the most significant health challenges of the 21st century, affecting the health of individuals globally. Approximately 830 million individuals across the globe are affected by diabetes, with a significant proportion residing in low- and middle-income nations [1]. The elevation of blood glucose levels leads to diabetes, resulting from a malfunction in insulin production. Various factors, including genetic tendencies and unhealthy lifestyle habits, can lead to this malfunction. Currently, unhealthy lifestyle choices play a major role in the rising incidence of diabetes [2]. Elevated blood glucose levels can result in vascular complications throughout the body, leading to a range of health issues. Diabetes has the potential to harm various organs, including the kidneys and eyes, and it also impacts nerve tissues and the cardiovascular system. Individuals diagnosed with diabetes face a heightened risk of experiencing heart attacks compared to those without the condition [3]. Diabetes is primarily classified into two types: insulin-dependent and non-insulin-dependent, commonly referred to as type 2 diabetes. The incidence of type 2 diabetes is frequently associated with obesity and a lack of physical activity [4]. Diabetes Mellitus is a chronic metabolic disorder marked by persistent hyperglycaemia, which occurs due to impairments in insulin secretion, insulin action, or both. This condition is linked to serious complications, including cardiovascular diseases, neuropathy, nephropathy, and retinopathy, all of which can significantly diminish the quality of life for those affected.

The management of diabetes focuses on controlling blood glucose levels through various therapeutic agents [5]. Among these, Thiazolidinediones (TZDs), also known as glitazones, represent a class of medications utilized in the treatment of type 2 diabetes. These medications function by activating peroxisome proliferator-activated receptors (PPARs), particularly PPARγ, which are nuclear receptors. This activation promotes the increased storage of fatty acids in adipocytes (fat cells), thereby decreasing the concentration of fatty acids in the bloodstream and enhancing cellular reliance on glucose for energy [6]. There are two drugs within this class that have received approval from the FDA including Pioglitazone and Rosiglitazone. These drugs may be administered independently or in conjunction with other oral medications for type 2 diabetes, including metformin or sulfonylureas. Nonetheless, they may lead to side effects such as weight gain and an increase in peripheral fat mass. Rosiglitazone (RGT) improves insulin sensitivity and glycaemic control by activating the PPARγ. PPAR-γ activation enhances insulin sensitivity in peripheral tissues, rendering it a viable treatment option for Type 2 Diabetes Mellitus [7]. However, many glitazone medications are classified as second-line treatments and exhibit significant toxicity. For

instance, while rosiglitazone was known to improve tissue sensitivity to insulin, it was banned in 2010 due to its association with heart failure. Additional serious side effects of this medication include blurred vision, numbness, bone fractures, respiratory tract infections, and strokes [8].

Bioisosteres represent a significant concept that has been widely utilized in the development of drugs and continues to be an essential strategic element in contemporary medicinal chemistry practices [9]. This concept involves the deliberate substitution of specific atoms or functional groups within a molecule with alternatives that possess comparable properties. This concept plays a crucial role in medicinal chemistry, enabling researchers to improve drug candidates by altering their pharmacological properties [10]. The objective may include enhancing metabolic stability or solubility while maintaining biological efficacy. Structural modifications classified as bioisosteres do not alter the biological function of the compound. Substitutions that involve changes to a compound's core are often termed scaffold hops, while those that modify the substituents of a core are typically referred to as functional group replacements [11,12]. Bioisosteres can be divided into classical and non-classical categories. classical bioisosteres involve the replacement of an atom or group with another that has similar dimensions, shape, and charge distribution. For example, substituting a hydrogen atom with a halogen atom (such as fluorine or chlorine) or an oxygen atom with a sulfur atom. Nonclassical bioisosteres involve more complex substitutions that may modify the electronic or steric properties of the molecule such as substituting a benzene ring with a thiophene ring [13,14]. The use of bioisosterism is particularly advantageous in addressing drug resistance, minimizing side effects, improving pharmacokinetic profile and enhancing drug-receptor interactions [15,16].The practice of substituting one part of a molecule with another that possesses comparable physical or chemical characteristics is a well-recognized approach in medicinal chemistry, aimed at enhancing drug features such as efficacy, selectivity, and safety [17-19].

This study concentrated on examining novel analogues of RGT to enhance the pharmacokinetic (ADME) profile and diminish toxicity, aiming to produce safer and more efficacious PPAR-γ activators for diabetes therapy.

2. Materials and Methods

2.1 Designing of Rosiglitazone Analogues

Authors have selected the pyridine group in the RGT molecule for the design of novel RGT analogues. A variety of bioisosteres of the pyridine group were generated by the MolOpt tool. This online web server facilitates in silico drug design by employing bioisosteric transformation rule. It assists medicinal chemists by automatically producing lists of analogues via bioisosteric replacement, which can subsequently be evaluated for potential synthesis. Additionally, it serves as a benchmark for appraising advancements in molecular optimization algorithms, with an emphasis on sample efficiency. The tool accommodates 25 molecular design algorithms across 23 tasks, rendering it a valuable resource for researchers and scientists [20,21].

2.2 Pharmacokinetic and Toxicological (ADMET) Profile Calculation

The produced analogues of RGT were subsequently utilized to calculate the ADMET profile employing the ADMETlab 3.0 online tool. It is an advanced tool within the field and a comprehensive software platform developed to prediction the absorption, distribution, metabolism, excretion, and toxicity characteristics of newly designed compounds [22,23]. This platform is a comprehensive online source containing eighty-four quantitative and four qualitative regression models that provide reliable and extensive predictions of ADMET properties for new ligands that mimic mammalian ADMET characteristics. It combines various computational models and databases to forecast the ADMET profiles of chemical compounds. This tool is important during the initial phases of drug discovery, as it aids in the identification of potential drug candidates with favourable ADMET properties [24,25]. By predicting the ADMET profiles of bioisosteric replacements, authors can choose the most promising candidates for subsequent screening studies.

2.3Drug Likeness (DL) and Drug Score (DS) Prediction

Drug likeness (DL) and drug score (DS) assessments play a crucial role in the initial stage of the drug development process. These evaluations aid researchers in identifying and prioritizing compounds, enabling them to focus on candidates with a higher likelihood of success in later development and clinical trials. The Osiris properties explorer (PEO) was utilized to compute DL and DS [26,27].

3. Results and Discussion

3.1 Designing of Analogues of Rosiglitazone

RGT serves as a second-line oral hypoglycaemic agent for managing diabetes mellitus. However, numerous patients have reported experiencing various toxicities associated with this medication. Therefore, it is essential to modify the structure of RGT to develop safer and less toxic analogues. MolOpt generated a total of 189 substitutable groups for the pyridine group within the RGT molecule (Figure 1). All 189 analogues were chosen for subsequent evaluations, including ADMET, DL, and DS predictions. After the screening, 46 selected analogues of RGT, along with their 2D structures are being shown in Table 1.MolOpt generates the variety of the bioisosteres for the pyridine group including pyrazole-3-amine, 2-(tert butyl)-4-methylthiazole, thiazole, n-cyclopropylformamide, cyclopropane-1-one, imidazolidine-2-one, 3-chorophenol, 6-methylpyridin-3-ol (Figure 2).

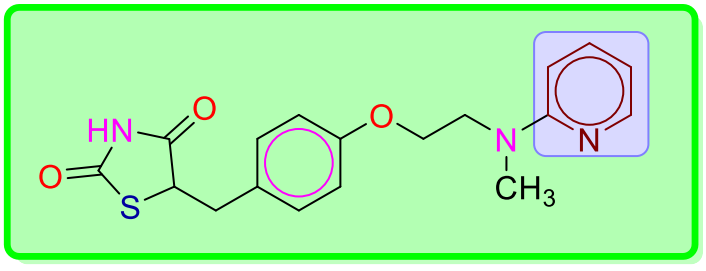

Figure 1. Structure of Rosiglitazone and its Modified Pyridine Group using Bioisosteric Approach.

S. No.	Entry no.	Smiles	MW	nHA	nHD	Log P	TPSA
STD	RGT	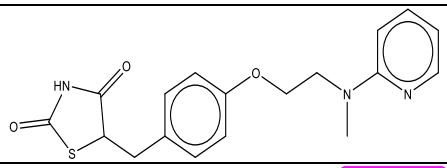	357.11	6	1	2.50	71.53
1	RGT01	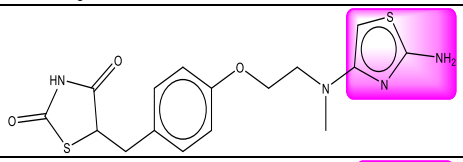	378.08	7	3	2.05	97.55
2	RGT02	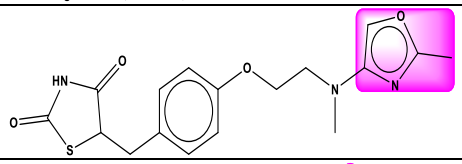	361.11	7	1	2.53	84.67
3	RGT03	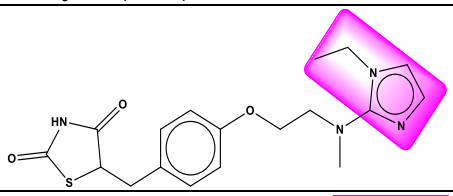	374.14	7	1	3.31	76.46
4	RGT04	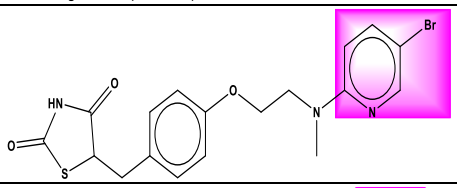	435.03	6	1	3.33	71.53
5	RGT05	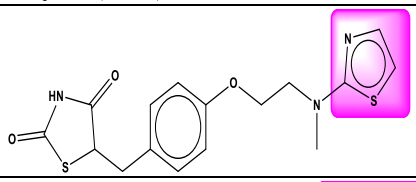	363.07	6	1	2.04	71.53
6	RGT06	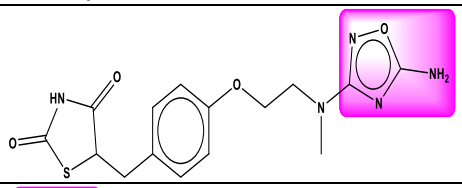	346.11	7	2	1.83	87.32
7	RGT07	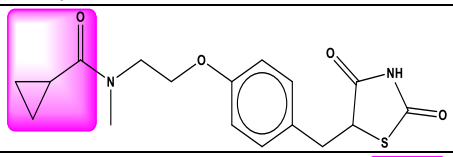	348.11	6	1	1.51	75.71
8	RGT08	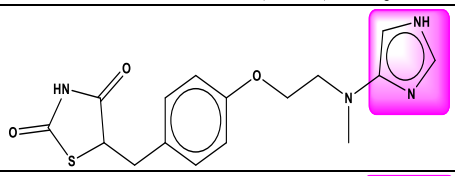	347.09	7	1	2.18	84.67
9	RGT09	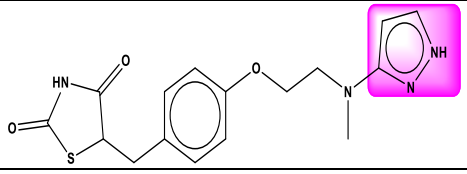	346.11	7	2	2.09	87.32

10	RGT010	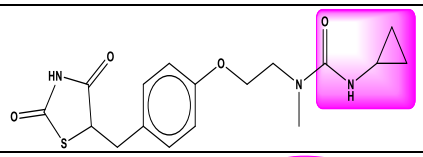	363.13	7	2	1.47	87.74
11	RGT011	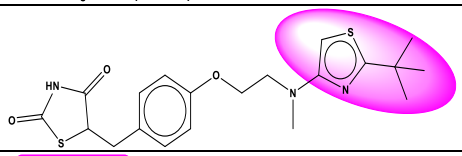	419.13	6	1	4.09	71.53
12	RGT012	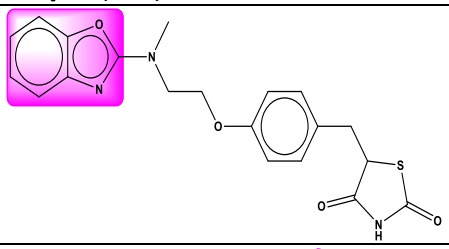	397.11	7	1	3.08	84.67
13	RGT013	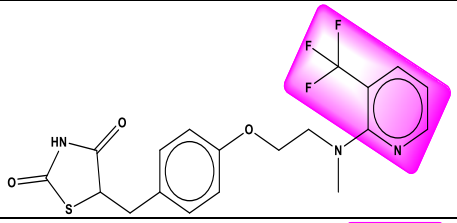	425.1	6	1	3.63	71.53
14	RGT014	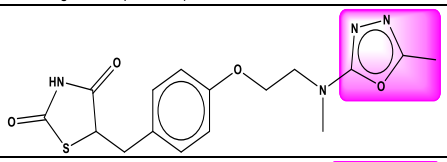	362.1	8	1	1.56	97.56
15	RGT015	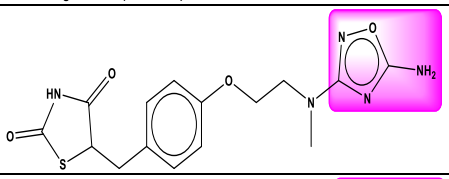	363.1	9	3	1.86	123.58
16	RGT016	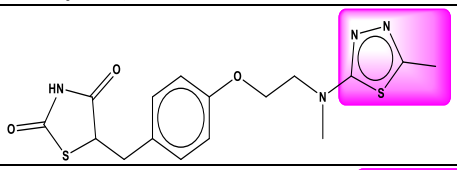	378.08	7	1	1.68	84.42
17	RGT017	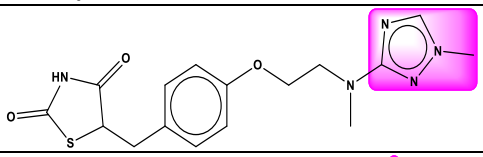	361.12	8	1	1.63	89.35
18	RGT018	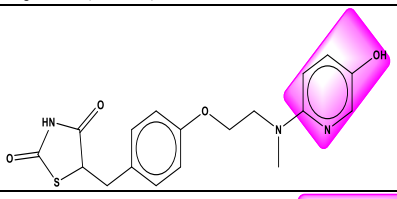	373.11	7	2	2.61	91.76
19	RGT019	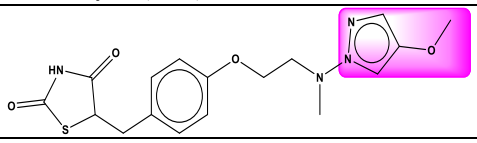	376.12	8	1	2.02	85.69

20	RGT020	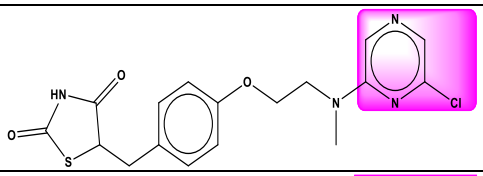	392.07	7	1	2.81	84.42
21	RGT021	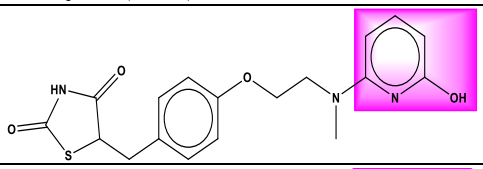	373.11	7	2	2.75	91.76
22	RGT0122	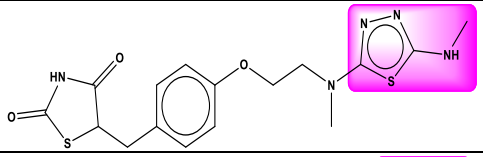	393.09	8	2	1.74	96.45
23	RGT023	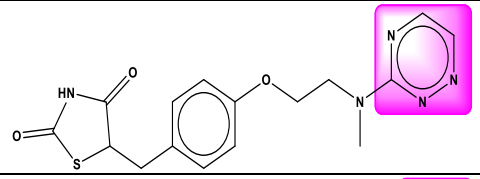	359.11	8	1	1.32	97.31
24	RGT024	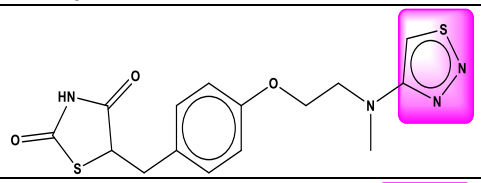	364.07	7	1	1.47	84.42
25	RGT025	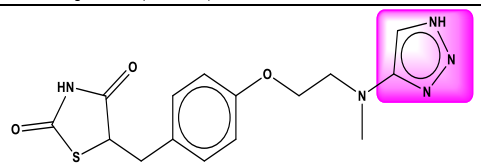	347.11	8	2	1.97	100.21
26	RGT026	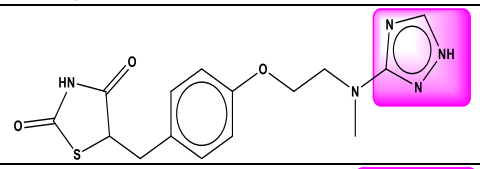	347.11	8	2	1.48	100.21
27	RGT027	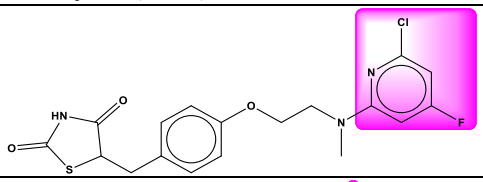	409.07	6	1	3.46	71.53
28	RGT028	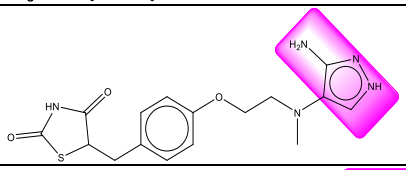	390.12	7	3	2.22	97.55
29	RGT029	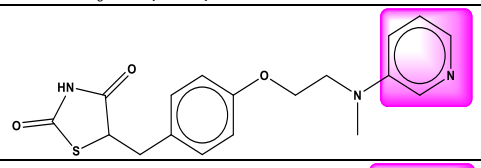	357.11	6	1	2.03	71.53
30	RGT030	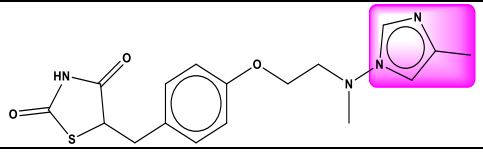	360.13	7	1	2.43	76.46

31	RGT031	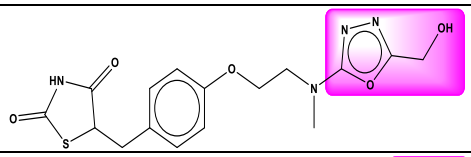	378.1	9	2	1.29	117.79
32	RGT032	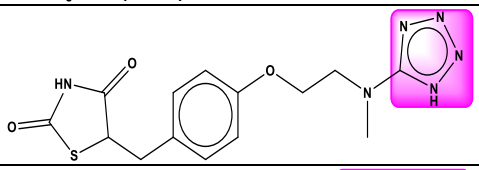	348.1	9	2	1.51	113.1
33	RGT033	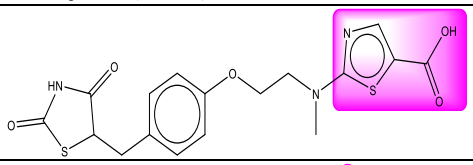	407.06	8	2	1.69	108.83
34	RGT034	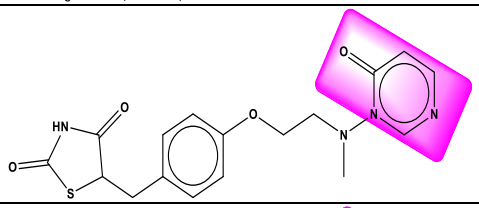	374.1	8	1	1.31	93.53
35	RGT035	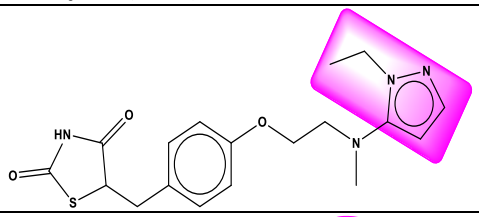	374.14	7	1	2.37	76.46
36	RGT036	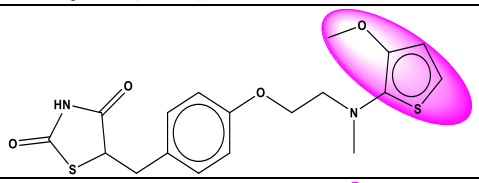	392.09	6	1	2.31	67.87
37	RGT037	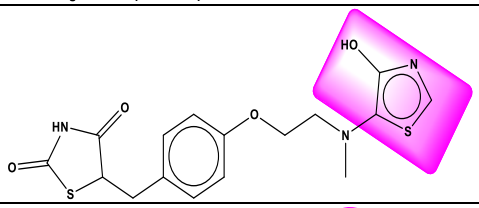	379.07	7	2	1.83	91.76
38	RGT038	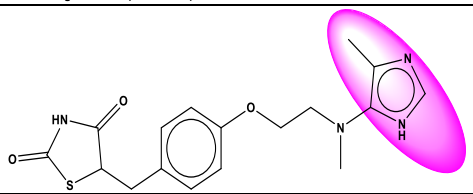	360.13	7	2	2.01	87.32
39	RGT039	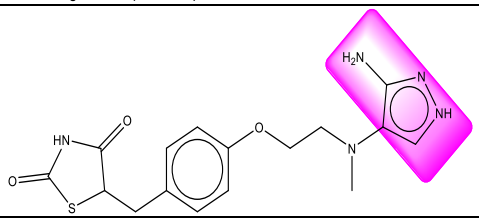	361.12	8	4	1.73	113.34
40	RGT040	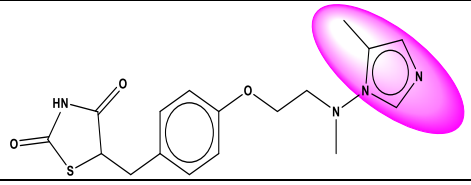	360.13	7	1	1.76	76.46

41	RGT041	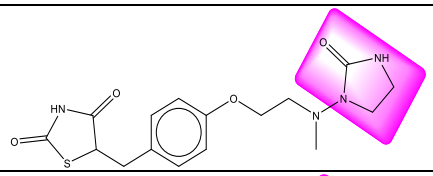	364.12	8	2	1.27	90.98
42	RGT042	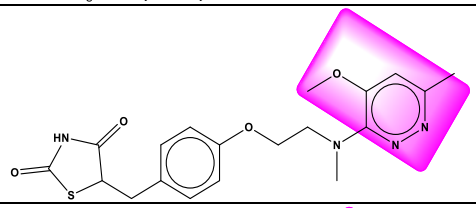	402.14	8	1	1.65	93.65
43	RGT043	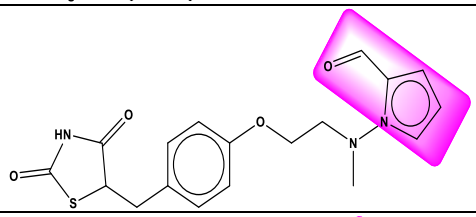	373.11	7	1	2.27	80.64
44	RGT044	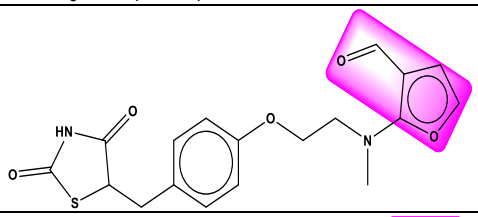	374.09	7	1	1.81	88.85
45	RGT045	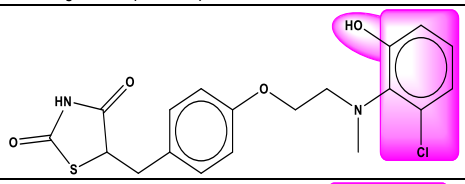	406.08	6	2	2.30	78.87
46	RGT046	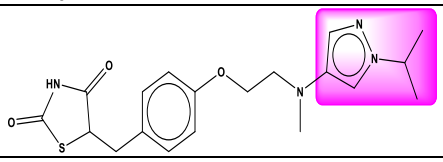	388.16	7	1	2.62	76.46

MW (Molecular weight), nHA (Number of hydrogen bond acceptor), nHD (Number of hydrogen bond donor), nRot (Number of rotatable bonds), TPSA (Topological polar surface area), logP (The logarithm of aqueous solubility value).

Table 1. Structure of the Rosiglitazone Analogues and their Physicochemical Properties

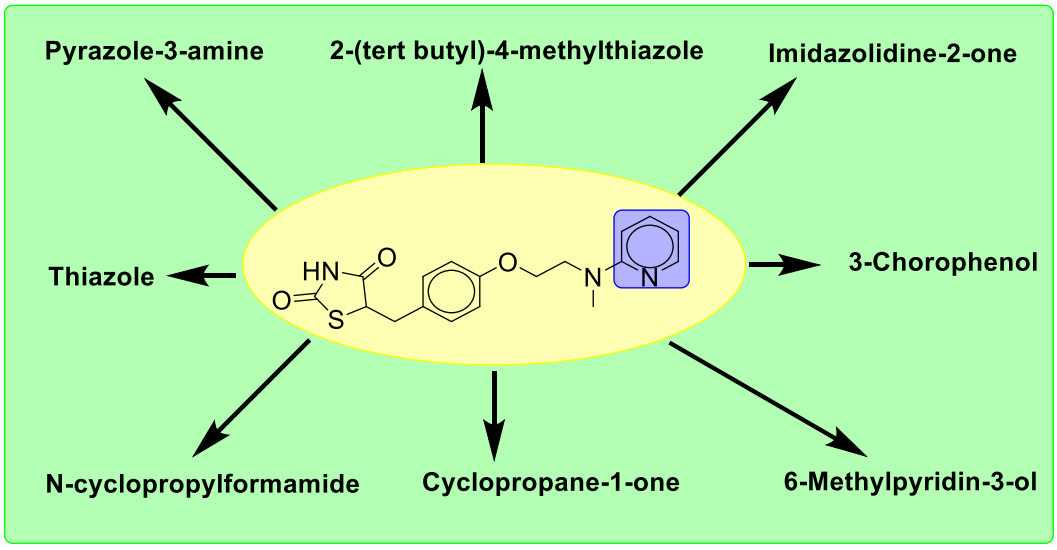

Figure 2: Variety of Pyridine Bioisosteres in the Rosiglitazone Molecule.

3.2 Calculation of Medicinal Profile

The medicinal properties of the designed analogues such as QED (Quantitative estimation of drug-likeness), SA (Synthetic accessibility), Fsp3 (The number of sp3 hybridized carbons/total carbon count), and MCE-18 (Medicinal chemistry evolution in 2018) has been carried out and their results are tabulated in Table 2. A QED, evaluates the drug-like characteristics of potential drug candidates. This assessment is grounded in desirability, which includes nine properties associated with drug likeness. The QED scores ofall designed analogues with exception of RGT012, fall within a favorable range (greater than 0.67), which was favourable as RGT (0.821). These scores indicate that all analogues represent attractive compounds as standard (RGT). The MCE-18 metric effectively evaluates the novelty of compounds based on their overall sp3 complexity. The MCE-18 scores ofall newly developed analogue found more than 45 indicatingsufficient novelty, necessitate visual examination to assess their target profiles and drug-likeness. Lipinski's rule has been satisfied by all analogues, indicating their potential for adequate absorption or permeability. Furthermore, Pfizer's criteria were also met by all analogues, suggesting favorable ADMET profiles. The Golden Triangle (GT) rule encompasses two parameters: molecular weight (MW) (≤200 and ≥50) and LogP (≤5 and ≥−2). All analogues complied with the acceptance criteria of the GT rule.

Entry no.	QED	SA	Fsp3	MCE-18	Lipinski	Pfizer	GSK	GT
STD	0.821	2.862	0.278	49.391	Accepted	Accepted	Accepted	Accepted
RGT01	0.762	3.213	0.312	52.619	Accepted	Accepted	Accepted	Accepted
RGT02	0.81	3.265	0.353	52.478	Accepted	Accepted	Accepted	Accepted
RGT03	0.764	3.183	0.389	52.36	Accepted	Accepted	Accepted	Accepted
RGT04	0.719	2.975	0.278	52.478	Accepted	Accepted	Accepted	Accepted
RGT05	0.815	3.055	0.312	49.524	Accepted	Accepted	Accepted	Accepted
RGT06	0.795	3.33	0.312	49.524	Accepted	Accepted	Accepted	Accepted
RGT07	0.814	2.827	0.471	56.44	Accepted	Accepted	Accepted	Accepted
RGT08	0.821	3.171	0.312	49.524	Accepted	Accepted	Accepted	Accepted
RGT09	0.795	3.366	0.312	49.524	Accepted	Accepted	Accepted	Accepted
RGT010	0.771	2.879	0.471	56.44	Accepted	Accepted	Accepted	Accepted
RGT011	0.735	3.31	0.45	61.379	Accepted	Accepted	Accepted	Accepted
RGT012	0.655	3.003	0.25	64.68	Accepted	Accepted	Accepted	Accepted
RGT013	0.732	3.097	0.316	61.6	Accepted	Accepted	Accepted	Accepted
RGT014	0.796	3.241	0.375	52.545	Accepted	Accepted	Accepted	Accepted
RGT015	0.743	3.334	0.333	52.7	Accepted	Accepted	Accepted	Accepted
RGT016	0.791	3.094	0.375	52.545	Accepted	Accepted	Accepted	Accepted
RGT017	0.793	3.261	0.375	52.545	Accepted	Accepted	Accepted	Accepted
RGT018	0.769	3.029	0.278	52.478	Accepted	Accepted	Accepted	Accepted
RGT019	0.746	3.458	0.353	52.478	Accepted	Accepted	Accepted	Accepted
RGT020	0.774	3.146	0.294	52.545	Accepted	Accepted	Accepted	Accepted
RGT021	0.769	3.163	0.278	52.478	Accepted	Accepted	Accepted	Accepted
RGT0122	0.703	3.19	0.375	52.545	Accepted	Accepted	Accepted	Accepted
RGT023	0.79	3.207	0.312	49.524	Accepted	Accepted	Accepted	Accepted
RGT024	0.804	3.33	0.333	49.6	Accepted	Accepted	Accepted	Accepted
RGT025	0.776	3.425	0.333	49.6	Accepted	Accepted	Accepted	Accepted
RGT026	0.776	3.455	0.333	49.6	Accepted	Accepted	Accepted	Accepted
RGT027	0.707	3.179	0.278	55.565	Accepted	Accepted	Accepted	Accepted
RGT028	0.748	3.173	0.278	55.565	Accepted	Accepted	Accepted	Accepted
RGT029	0.821	2.887	0.278	49.391	Accepted	Accepted	Accepted	Accepted
RGT030	0.81	3.41	0.353	52.478	Accepted	Accepted	Accepted	Accepted
RGT031	0.693	3.349	0.375	52.545	Accepted	Accepted	Accepted	Accepted
RGT032	0.748	3.412	0.357	49.684	Accepted	Accepted	Accepted	Accepted
RGT033	0.686	3.144	0.294	55.636	Accepted	Accepted	Accepted	Accepted
RGT034	0.766	3.379	0.294	52.545	Accepted	Accepted	Accepted	Accepted
RGT035	0.764	3.226	0.389	52.36	Accepted	Accepted	Accepted	Accepted
RGT036	0.744	3.198	0.333	52.417	Accepted	Accepted	Accepted	Accepted
RGT037	0.762	3.447	0.312	52.619	Accepted	Accepted	Accepted	Accepted
RGT038	0.786	3.339	0.353	52.478	Accepted	Accepted	Accepted	Accepted
RGT039	0.683	3.405	0.312	52.619	Accepted	Accepted	Accepted	Accepted
RGT040	0.81	3.418	0.353	52.478	Accepted	Accepted	Accepted	Accepted
RGT041	0.745	3.379	0.438	55.435	Accepted	Accepted	Accepted	Accepted
RGT042	0.718	3.191	0.368	55.385	Accepted	Accepted	Accepted	Accepted
RGT043	0.711	3.434	0.278	52.478	Accepted	Accepted	Accepted	Accepted
RGT044	0.71	3.364	0.278	52.478	Accepted	Accepted	Accepted	Accepted
RGT045	0.733	3.032	0.263	55.5	Accepted	Accepted	Accepted	Accepted
RGT046	0.749	3.236	0.421	55.333	Accepted	Accepted	Accepted	Accepted

QED (Quantitative estimation of drug-likeness), SA (Synthetic accessibility score), Fsp3 (The number of sp3 hybridized carbons/total carbon count), MCE-18 (Medicinal chemistry evolution in 2018), GSK (GlaxoSmithKline), GT (Golden Triangle)

Table 2. Medicinal Properties of Rosiglitazone Analogues.

3.3 Prediction of Pharmacokinetic (ADME) Properties

Pharmacokinetic parameters play a vital role in the development of new drugs, as they provide critical information regarding the absorption, distribution, metabolism, and excretion of a drug within the human body. The pharmacokinetic parameters, which encompass absorption (Caco-2, MDCK, and HIA), distribution (BBB, PPB, and VD), metabolism (CYP1A2), and excretion (CL and $T_{1/2}$), have been calculated for the designed analogues, with their respective scores tabulated in Table 3. The Caco-2 (human colon adenocarcinoma cell line) is a commonly used in vitro model for predicting the intestinal permeability of drugs and evaluating their potential for oral absorption. Consequently, the evaluation of permeability through Caco-2 cells has become a significant factor in assessing the viability of a therapeutic compound. The results indicate that the Caco-2 scores for analogues RGT04, RGT05, RGT011, RGT012, RGT013, RGT014, RGT16, RGT020, RGT036, and RGT042 found more than -5.15, suggesting favorable in vivo drug permeability. A strong MDCK score further implies that all analogues possess the capability to permeate and traverse cellular membranes. Human intestinal absorption (HIA) scores ranging from 0 to 0.3 suggest that these analogues may exhibit good oral bioavailability. The blood-brain barrier (BBB) scores for analogues RGT01-046 are below 0.03, indicating a potential safety profile against central nervous system side effects. Furthermore, the designed analogues, including RGT01-046, demonstrate poor plasma protein binding (PPB) of less than 90%, suggesting limited distribution throughout the body. The volume of distribution (VD) scores for all analogues falls between 0.04 and 20, indicating an adequate distribution in body fluids and tissue uptake. Cytochrome P450 (CYP P450), a family of isozymes, is essential for phase-I and phase-II drug metabolism. All analogues exhibit a high substrate score and a low inhibitor score for CYP1A2.Metabolism (CYP1A2-inh and sub, CYP2C19-inh and sub, CYP2C9-inh and sub, CYP2D6-inh and sub, CYP3A4-inh and sub), clearance and half-life ($T_{1/2}$) scores were calculated and their results are shown in Table4.

Entry no.	Caco2	MDCK	PAMPA	HIA	BBB	PPB	FU
STD	-4.663	0.819	0.055	0.001	99.426	0.250	0.859
RGT01	-5.186	-4.940	0.895	0.187	0.001	98.962	0.821
RGT02	-5.161	-4.517	0.871	0.005	0.001	98.867	0.829
RGT03	-5.276	-4.815	0.181	0.020	0.004	99.378	0.284
RGT04	-4.866	-4.466	0.874	0.010	0.048	99.285	0.486
RGT05	-4.737	-4.382	0.899	0.229	0.001	99.462	0.237
RGT06	-5.252	-4.891	0.889	0.129	0.000	98.954	0.731
RGT07	-5.155	-4.661	0.971	0.378	0.000	98.509	0.763
RGT08	-5.134	-4.563	0.893	0.185	0.001	98.875	0.761
RGT09	-5.182	-4.733	0.921	0.177	0.001	99.343	0.379
RGT010	-5.309	-4.744	0.986	0.551	0.000	99.023	0.602
RGT011	-4.963	-4.484	0.777	0.276	0.000	99.646	0.198
RGT012	-5.090	-4.607	0.755	0.004	0.018	99.409	0.254
RGT013	-5.096	-4.769	0.788	0.021	0.005	99.576	0.254
RGT014	-5.057	-4.519	0.812	0.002	0.003	98.755	1.374
RGT015	-5.313	-4.860	0.948	0.002	0.001	98.924	0.888
RGT016	-4.895	-4.537	0.937	0.014	0.002	98.709	1.059
RGT017	-5.120	-4.464	0.890	0.004	0.002	98.973	0.715
RGT018	-5.347	-4.721	0.979	0.075	0.000	99.359	0.337
RGT019	-5.044	-4.406	0.731	0.177	0.000	99.411	0.393
RGT020	-4.801	-4.686	0.925	0.044	0.001	99.038	0.581
RGT021	-5.414	-4.715	0.976	0.220	0.000	98.882	0.730
RGT0122	-5.132	-4.994	0.926	0.226	0.001	98.991	0.591
RGT023	-5.122	-4.462	0.896	0.024	0.003	98.971	0.692
RGT024	-5.030	-4.391	0.918	0.345	0.001	99.336	0.334
RGT025	-5.255	-4.693	0.956	0.419	0.000	99.159	0.560
RGT026	-5.164	-4.645	0.931	0.040	0.001	99.306	0.349
RGT027	-5.099	-4.620	0.542	0.001	0.000	99.479	0.326
RGT028	-5.187	-4.658	0.683	0.001	0.000	99.201	0.854
RGT029	-5.130	-4.681	0.830	0.102	0.000	98.853	0.976
RGT030	-5.131	-4.613	0.734	0.012	0.000	98.662	1.237
RGT031	-5.659	-4.750	0.893	0.069	0.001	99.101	1.372
RGT032	-5.209	-4.729	0.970	0.737	0.000	99.053	0.743
RGT033	-5.786	-5.038	0.998	0.474	0.000	99.395	0.248
RGT034	-5.121	-4.820	0.949	0.101	0.000	98.966	1.220
RGT035	-5.369	-4.776	0.478	0.051	0.018	99.115	0.673
RGT036	-4.952	-4.301	0.797	0.211	0.001	99.381	0.350
RGT037	-5.222	-4.683	0.949	0.327	0.001	98.949	0.597
RGT038	-5.177	-4.814	0.940	0.035	0.002	99.245	0.624
RGT039	-5.488	-5.047	0.918	0.157	0.001	99.407	1.231
RGT040	-5.040	-4.743	0.911	0.038	0.001	98.373	1.953
RGT041	-5.346	-4.949	0.950	0.571	0.002	98.718	1.451
RGT042	-4.973	-4.633	0.168	0.003	0.001	98.838	1.044
RGT043	-5.413	-4.829	0.871	0.175	0.001	99.389	0.376
RGT044	-5.301	-4.898	0.879	0.329	0.001	99.436	0.297

RGT045	-5.369	-4.779	0.794	0.040	0.002	99.403	0.303
RGT046	-5.018	-4.894	0.380	0.093	0.000	99.148	0.522

Caco2 (Human colon adenocarcinoma cell line), MDCK (Madin−Darby Canine Kidney cells), PAMPA (The Parallel Artificial Membrane Permeability Assay), HIA (Human intestinal absorption), BBB (Blood Brain Barrier), PPB (Plasma protein binding), FU (Fraction Unbound).

Table 3: Absorption and Distribution Profile of the Analogues.

Entry No.	CYP1A2	CYP2C19	CYP2C9	CYP3A4	CYP2B6	CYP2C8	CL	$T_{1/2}$
RGT01	+	+	+	+	+	+	7.656	1.221
RGT02	-	+	+	+	+	+	6.771	1.031
RGT03	-	+	+	+	+	+	7.297	0.794
RGT04	+	+	+	+	+	+	6.303	1.159
RGT05	-	+	+	+	+	+	6.204	0.809
RGT06	+	+	+	+	+	+	7.846	1.148
RGT07	+	+	+	+	+	+	7.789	1.112
RGT08	+	+	+	+	+	+	7.954	1.151
RGT09	+	+	+	+	+	+	8.145	1.169
RGT010	+	+	+	+	+	+	8.280	1.117
RGT011	+	+	+	+	+	+	5.520	0.618
RGT012	+	+	+	+	+	+	4.559	0.727
RGT013	-	+	+	+	+	+	7.419	0.811
RGT014	-	+	+	+	+	+	4.979	1.054
RGT015	+	+	+	+	+	+	6.611	1.180
RGT016	-	+	+	+	+	+	4.420	0.780
RGT017	-	+	+	+	+	+	5.064	0.936
RGT018	-	+	+	+	+	+	7.865	1.098
RGT019	-	+	+	+	+	+	7.846	1.086
RGT020	+	+	+	+	+	+	7.279	1.172
RGT021	+	+	+	+	+	+	7.308	1.165
RGT0122	-	+	+	+	+	+	4.985	1.094
RGT023	-	+	+	+	+	+	6.006	0.922
RGT024	+	+	+	+	+	+	7.030	0.889
RGT025	-	+	+	+	+	+	7.601	0.929
RGT026	-	+	+	+	+	+	6.574	1.025
RGT027	+	+	+	+	+	+	6.240	0.908
RGT028	+	+	+	+	+	+	7.698	1.249
RGT029	-	-	+	+	+	+	7.925	0.799
RGT030	-	+	+	+	+	+	7.860	0.813
RGT031	-	+	+	+	+	+	6.176	1.029
RGT032	-	+	+	+	+	+	7.305	1.076
RGT033	+	+	+	+	+	+	3.965	1.200
RGT034	-	+	+	+	+	+	7.388	1.089
RGT035	-	+	+	+	+	+	7.672	0.799
RGT036	-	+	+	+	+	+	7.142	0.575
RGT037	-	+	+	+	+	+	5.711	0.936
RGT038	-	+	+	+	+	+	7.389	0.784
RGT039	+	+	+	+	+	+	7.482	1.224
RGT040	+	+	+	+	+	+	6.415	0.677
RGT041	+	+	+	+	+	+	8.010	1.515
RGT042	-	+	+	+	+	+	6.074	0.812
RGT043	-	+	+	+	+	+	7.395	0.928
RGT044	-	+	+	+	+	+	6.265	1.056
RGT045	-	+	+	+	+	+	5.540	0.866
RGT046	+	+	+	+	+	+	8.410	0.776

Human cytochrome P450 (five isozymes—1A2, 3A4, 2C9, 2C19 and 2D6), + (indicates the compound act as substrate against the isozymes), - (indicates the compound act as inhibitor against the isozymes), CL (The clearance of a drug), $T_{1/2}$ (The half-life of a drug).

Table 4: Metabolism and Excretion profile Prediction of the Analogues

3.4 Prediction of the toxicity properties

The assessment of the toxicological characteristics of the analogues was conducted, focusing on various parameters such as drug-induced liver injury (DILI), mutagenicity as determined by the Ames test, acute oral toxicity in rats (ROA), the interaction of the molecule with the ligand-binding domain (LBD) of the androgen receptor (NR-AR-LBD), and carcinogenic potential. The results of these evaluations are presented in Table 3. Notably, all designed analogues exhibited identical human hepatotoxicity (H-HT) scores to RGT01-046, suggesting a potential for mild toxicity, with scores ranging from 0.3 to 0.7. In contrast, RGT04, RGT018, and RGT022 were predicted to have a safer DILI score, falling between 0 and 0.3, indicating lower toxicity levels. However, RGT01,

RGT28, RGT30, and RGT043 were anticipated to exhibit higher toxicity in the Ames test. The toxicity profile of the analogues with their score is shown in Table 5.

3.5 Prediction of DS and DL score

The definitions of Druglikeness (DL) and Drug Score (DS) have been formulated based on specific physicochemical characteristics of established drug compounds and their impact on molecular behavior in vitro. The DL and DS metrics are predictive of various properties, including solubility, permeability, metabolic stability, and transporter interactions, relevant to drug candidates. The DL score of these compounds may offer insights into their safety and effectiveness. Conversely, the DS serves as a holistic measure that integrates various attributes such as druglikeness, cLogP, logS, molecular weight (MW), and toxicity issues into a singular value. This metric can be utilized to evaluate the likelihood of an unknown compound fulfilling the necessary criteria to qualify as a drug [28,29]. Among all analogues, RGT46 exhibits the highest DL score, followed by others. The DL and DS scores of the analogues with their score is shown in Table 5.

Entry no.	H-HT	DILI	hERG	Ames	ROA	NR-AR	DL	DS
	0.393	0.969	0.198	0.172	0.158	0.001	9.14	0.8
RGT01	0.689	1.000	0.179	0.743	0.274	0.002	8.59	0.74
RGT02	0.514	0.994	0.191	0.517	0.327	0.002	5.99	0.64
RGT03	0.503	0.998	0.252	0.419	0.235	0.001	5.99	0.62
RGT04	0.322	0.992	0.237	0.114	0.226	0.002	10.92	0.84
RGT05	0.481	0.999	0.177	0.467	0.259	0.001	9.97	0.8
RGT06	0.508	0.998	0.162	0.480	0.267	0.001	9.2	0.81
RGT07	0.531	0.982	0.285	0.450	0.223	0.002	9.63	0.85
RGT08	0.524	0.998	0.236	0.449	0.324	0.004	0.85	0.84
RGT09	0.502	0.998	0.142	0.425	0.162	0.001	0.52	0.84
RGT010	0.565	0.992	0.173	0.388	0.271	0.001	0.53	0.84
RGT011	0.565	0.999	0.237	0.518	0.232	0.000	0.87	0.79
RGT012	0.519	0.996	0.243	0.536	0.243	0.003	1.49	0.6
RGT013	0.583	0.993	0.296	0.261	0.311	0.001	8.3	0.78
RGT014	0.572	0.995	0.135	0.533	0.314	0.001	8.73	0.69
RGT015	0.634	0.999	0.144	0.659	0.315	0.002	8.99	0.68
RGT016	0.504	0.996	0.157	0.500	0.248	0.000	4.19	0.76
RGT017	0.592	0.997	0.134	0.692	0.196	0.000	5.39	0.67
RGT018	0.391	0.955	0.201	0.283	0.156	0.004	8.29	0.87
RGT019	0.481	0.995	0.159	0.690	0.236	0.001	6.41	0.39
RGT020	0.453	0.996	0.286	0.336	0.357	0.000	4.49	0.86
RGT021	0.360	0.967	0.089	0.250	0.168	0.000	8.74	0.82
RGT0122	0.455	0.997	0.180	0.615	0.393	0.000	10.36	0.84
RGT023	0.406	0.990	0.180	0.372	0.295	0.000	9.88	0.86
RGT024	0.526	0.998	0.212	0.631	0.291	0.001	8.87	0.51
RGT025	0.341	0.986	0.160	0.458	0.257	0.000	8.39	0.81
RGT026	0.558	0.999	0.124	0.520	0.178	0.000	8.97	0.5
RGT027	0.542	0.992	0.292	0.403	0.416	0.000	6.05	0.58
RGT028	0.493	0.995	0.290	0.786	0.346	0.003	7.79	0.85
RGT029	0.327	0.994	0.212	0.301	0.264	0.001	9.24	0.83
RGT030	0.459	0.999	0.178	0.716	0.222	0.001	7.21	0.86
RGT031	0.506	0.995	0.097	0.571	0.206	0.002	9.59	0.76
RGT032	0.480	0.990	0.124	0.429	0.334	0.000	8.3	0.82
RGT033	0.462	0.999	0.076	0.381	0.153	0.001	9.29	0.87
RGT034	0.458	0.999	0.120	0.661	0.229	0.000	7.59	0.67
RGT035	0.425	0.988	0.242	0.482	0.265	0.000	8.9	0.85
RGT036	0.478	0.999	0.270	0.502	0.206	0.001	9.4	0.83
RGT037	0.436	0.998	0.088	0.406	0.248	0.000	6.5	0.65
RGT038	0.570	0.997	0.178	0.442	0.444	0.004	8.3	0.62
RGT039	0.475	0.996	0.203	0.612	0.269	0.000	9.56	0.87
RGT040	0.521	0.999	0.152	0.694	0.256	0.001	8.33	0.8
RGT041	0.435	0.992	0.274	0.642	0.365	0.001	9.13	0.78
RGT042	0.445	0.987	0.202	0.525	0.282	0.000	8.82	0.76
RGT043	0.373	0.998	0.113	0.709	0.159	0.000	9.25	0.74
RGT044	0.342	0.995	0.173	0.345	0.228	0.000	9.73	0.86
RGT045	0.385	0.997	0.140	0.403	0.180	0.001	6.94	0.76
RGT046	0.519	0.995	0.224	0.430	0.229	0.000	9.68	0.89

H-HT (The human hepatotoxicity), DILI (Drug-induced liver injury), hERG (Human ether-a-go-go related gene or cardiotoxicity), Ames (test for mutagenicity), ROA (Rat Oral Acute Toxicity, NR-AR (Nuclear receptor-androgen receptor), DL (drug likeness), DS (Drug score).

Table 5. Toxicity, Drug Likness and Drug Score Prediction of Design Analogues

4. Conclusion

Diabetes is a major global health concern, primarily arising from insulin dysfunction, genetic factors, and unhealthy lifestyle choices, leading to elevated blood glucose levels and an increasing incidence of the disease. Rosiglitazone, a PPAR-γ agonist used in the treatment of Type 2 Diabetes Mellitus, was removed from the market in 2010 due to its association with heart failure. Additionally, this medication is linked to serious side effects, such as blurred vision, numbness, bone fractures, respiratory infections, and strokes. In medicinal chemistry, the principle of bioisosterism involves substituting a part of a molecule with another that has comparable physical or chemical characteristics, thereby enhancing the drug's efficacy, selectivity, and safety. This research aims to explore new analogues of Rosiglitazone to improve the pharmacokinetic profile (ADME) and minimize toxicity, with the objective of developing safer and more effective PPAR-γ activators for diabetes management. A total of 191 pyridine bioisosteres, including thiazolidine, phenoxy, and methoxyphenyl, were generated using the MolOpt tool. The newly synthesized compounds were assessed for their medicinal properties, pharmacokinetic (ADME) parameters, and toxicity profiles through the ADMETLab 3.0 online platform. The distribution of lipophilicity (DL) and solubility (DS) was evaluated using PEO calculations. After the screening process, 46 analogues exhibited favorable drug-likeness, QED scores, and adherence to Lipinski's rule. Notable candidates identified include compounds RGT008, RGT029, RGT04, RGT05, RGT010, and RGT011, which were distinguished based on their QED and MCE-18 scores. Moreover, compounds RGT011 and RGT021 demonstrated reduced hepatotoxicity and cardiac toxicity compared to the standard (RGT). The comprehensive analysis indicates that compounds RGT05, RGT04, and RGT021 merit further exploration as potential PPAR-γ activators, suggesting their potential as anti-diabetic agents.

Conflict of Interest

The authors have no conflicts of interest regarding this investigation.

Acknowledgements

The authors wish to thank the Head, Department of Pharmacy, Guru Ghasidas Vishwavidyalaya, Bilaspur (CG) for providing necessary facilities to carry out the research work.

References

1. Sun H, Saeedi P, Karuranga S, Pinkepank M, Ogurtsova K, Duncan BB, et al. (2022). IDF Diabetes Atlas: Global, regional and country-level diabetes prevalence estimates for 2021 and projections for 2045. Diabetes Research and Clinical Practice. 183: 109-119.
2. Banday MZ, Sameer AS, Nissar S. (2020). Pathophysiology of diabetes: An overview. Avicenna journal of medicine. 10(04): 174-188.
3. Galicia-Garcia U, Benito-Vicente A, Jebari S, Larrea-Sebal A, Siddiqi H, Uribe KB, et al. (2020). Pathophysiology of type 2 diabetes mellitus. International journal of molecular sciences. 21(17): 6275.
4. Baynes HW. (2015). Classification, pathophysiology, diagnosis and management of diabetes mellitus. J diabetes metab. 2015; 6(5): 1-9.
5. O'Kell AL, Davison LJ. (2023). Etiology and pathophysiology of diabetes mellitus in dogs. Veterinary Clinics: Small Animal Practice. 53(3): 493-510.
6. Xiong G, Wu Z, Yi J, Fu L, Yang Z, Hsieh C, Yin M, Zeng X, Wu C, Lu A, Chen X, Hou T, Cao D. (2021). ADMETlab 2.0: an integrated online platform for accurate and comprehensive predictions of ADMET properties. Nucleic Acids Res. 2(49): 14.
7. Dong, J., Wang, NN., Yao, ZJ. et al. (2018). ADMETlab: a platform for systematic ADMET evaluation based on a comprehensively collected ADMET database. Journal of Cheminformatics. 10: 29
8. Ismail, Noor Zafirah & Annamalai, Nithyanan & Mohamad Zain, Nur Nadhirah&Arsad, Hasni. (2020). molecular docking of selected compounds from clinacanthus nutans with bcl-2, p53, caspase-3 and caspase-8 proteins in the apoptosis pathway. Journal of Biological & Scientific Opinion. 8: 4-11.
9. Jiang B, Luo J, Guo S, Wang L. (2021). Discovery of 5-(3-bromo-2-(2, 3-dibromo-4, 5-dimethoxybenzyl)-4, 5-dimethoxybenzylidene) thiazolidine-2, 4-dione as a novel potent protein tyrosine phosphatase 1B inhibitor with antidiabetic properties. Bioorganic Chemistry. 108: 104648.
10. Senthilkumar N, Vijayakumar V, Sarveswari S, Gayathri GA, Gayathri M. (2021). Synthesis of new thiazolidine-2,-4-dione-azole derivatives and evaluation of their α-amylase and α-glucosidase inhibitory activity. Iranian Journal of Science and Technology, Transactions A: Science. 43: 735-745.
11. Meanwell NA. (2014). The Influence of Bioisosteres in Drug Design: Tactical Applications to Address Developability Problems. Tactics in Contemporary Drug Design. 9: 283-381.
12. G. Papadatos, M. Alkarouri, V. J. Gillet, P. Willett, V. Kadirkamanathan, C. N. Luscombe, G. Bravi, N. J. Richmond, S. D. Pickett, J. Hussain, J. M. Pritchard, A. W. J. Cooper, S. J. F. Macdonald, J. Chem. Inf. Model. (2010). 50, 1872-1886;
13. Ali, G., Subhan, F., Rauf, K., Samiullah, Islam, N.U., Khan, I., Abbas, M., & Rauf, A. (2012). Input of Isosteric and Bioisosteric Approach in Drug design. Journal of the Chemical Society of Pakistan, 36, 150-169.
14. Vink, G., Nebel, J. C., & Wren, S. P. (2021). In Silico Design of Bioisosteric Modifications of Drugs for the Treatment of Diabetes. Future Medicinal Chemistry, 13(8), 691-700.
15. G. Papadatos, M. Alkarouri, V. J. Gillet, P. Willett, V. Kadirkamanathan, C. N. Luscombe, G. Bravi, N. J. Richmond, S. D. Pickett, J. (2010). Hussain, J. M. Pritchard, A. W. J. Cooper, S. J. F. Macdonald, J. Chem. Inf. Model. 50: 1872-1886;
16. Vink G, Nebel JC, Wren SP. In Silico Design of Bioisosteric Modifications of Drugs for the Treatment of Diabetes. Future Medicinal Chemistry, 2021; 13(8): 691–700.
17. https://www.tandfonline.com/doi/abs/10.1080/07391102.2023.2256887
18. Ertl P, Schuffenhauer A. (2009). Estimation of syenthetic accessibility score of drug-like molecules based on molecular complexity and fragment contributions[J]. J cheminform, 1(1): 8.
19. Yu J, Wang J, Zhao H, et al. (2022). Organic Compound Synthetic Accessibility Prediction Based on the Graph Attention Mechanism. J Chem Inf Model. 62(12): 2973-2986.
20. Shan J, Ji C. (2020). MolOpt: a web server for drug design using bioisosteric transformation. Current computer-aided drug design. Aug 1;16(4):460-466.
21. Modee R, Mehta S, Laghuvarapu S, Priyakumar UD. (2023). MolOpt: autonomous molecular geometry optimization using multiagent reinforcement learning. The Journal of Physical Chemistry B. 127(48):10 295-303.
22. Fu L, Shi S, Yi J, Wang N, He Y, Wu Z, Peng J, Deng Y, Wang W, Wu C, Lyu A. (2023). ADMETlab 3.0: an updated comprehensive online ADMET prediction platform enhanced with broader coverage, improved performance, API functionality and decision support. Nucleic acids research. 52(W1): 422-431.
23. Srinivasa MG, Paithankar JG, Birangal SR, Pai A, Pai V, Deshpande SN, Revanasiddappa BC. (2023). Novel hybrids of thiazolidinedione-1, 3, 4-oxadiazole derivatives: synthesis, molecular docking, MD simulations, ADMET study, in vitro,

and in vivo anti-diabetic assessment. RSC advances. 13(3):1567-79.
24. Xiong G, Wu Z, Yi J, Fu L, Yang Z, Hsieh C, Yin M, Zeng X, Wu C, Lu A, Chen X. (2023). ADMETlab 2.0: an integrated online platform for accurate and comprehensive predictions of ADMET properties. Nucleic acids research. (W1):5-14.
25. Kumar TA, Kabilan S, Parthasarathy V. (2017). Screening and toxicity risk assessment of selected compounds to target cancer using QSAR and pharmacophore modelling. international journal of PharmTech Research. 2017; 10(4): 219-224.
26. Sander T,Freyss J, Korff MV, Reich JR, RufenerC. (2009). OSIRIS, an Entirely in-House Developed Drug Discovery Informatics System. J. Chem. Inf. Model. 49(2): 232-246.
27. Sander T. (2001). OSIRIS Property Explorer. Organic Chemistry Portal.
28. Bickerton GR, Paolini GV, Besnard J, Muresan S, Hopkins AL. (2012). Quantifying the chemical beauty of drugs. Nat Chem. 4(2):90-98.
29. Sun J, Wen M, Wang H, Ruan Y, Yang Q, Kang X, et al. (2012). Prediction of drug-likeness using graph convolutional attention network. Bioinformatics. 38(23):5262-5269.

DOI:10.31579/2767-7370/150